Ind. J. Pharm. Edu. Res., 2025; 59(4):1522-1533.
https://www.ijper.org

Original Article

In silico and *in vivo* Evaluation of Antitumor Drugs against *P. falciparum* 3D7 Inhibit the Parasite Growth

Mohammad Aatif[1], Mohd Farhan[2,3], Ghazala Muteeb[4,*]

[1]Department of Public Health, College of Applied Medical Sciences, King Faisal University, Al Ahsa, SAUDI ARABIA.
[2]Department of Basic Sciences, Preparatory Year, King Faisal University, Al Ahsa, SAUDI ARABIA.
[3]Department of Chemistry, College of Science, King Faisal University, Al Ahsa, SAUDI ARABIA.
[4]Department of Nursing, College of Applied Medical Sciences, King Faisal University, Al Ahsa, SAUDI ARABIA.

ABSTRACT

Background: *Plasmodium falciparum* (*P. falciparum*) is the most lethal parasite that affectsmalaria in humans. The drugs such as Etoposide, Novobiocin, Netropsin, Nogalamycin and Daunorubicin may be useful in treating such diseases. Here, molecular docking study predicts the novel drug candidate. Further, computational and *in vivo* of the pharmacokinetic properties also helps to predict the drug candidate. **Materials and Methods:** At first, we optimized five antitumor drugs Etoposide, Novobiocin, Netropsin, Nogalamycin and Daunorubicin then analyze the frontier molecular orbitals followed by molecular docking against the target protein {PF3D7_1441900 (transcription factor TFIIH complex subunit Tfb5, putative) *P. falciparum* (isolate 3D7)}. Pharmacokinetic properties calculated by using the ADMET 2.0. We used SYBR green dye assess anti-malarial drugs (Etoposide, Novobiocin, Netropsin, Nogalamycin and Daunorubicin) against the malaria parasite 3D7 based on the fluorescence assay. **Results:** Our calculations show that all the studied drugs Etoposide, Novobiocin, Netropsin, Nogalamycin and Daunorubicin can have an affinity with the *Plasmodium falciparum* (isolate 3D7)}. ADME computed permeability, distribution, and metabolism characteristics of the drugs. We found in our *in vivo* 7 *in silico* study that Novobiocin and etoposide are valuable and maximum inhibition of the parasite *P. falciparum* 3D7 strain growth in comparison to others. **Conclusion:** Our study concluded that Etoposide and Novobiocin could illustration the better affinity with the protein *Plasmodium falciparum*. The ADME analysis can be used for evaluating the pharmacokinetic properties. Novobiocin is possible inhibitor for malaria.

Keywords: *Plasmodium falciparum*, Drugs, FMO, DFT, Molecular Docking, ADME. Inhibition, Parasite growth.

Correspondence:
Dr. Ghazala Muteeb
Department of Nursing, College of Applied Medical Sciences, King Faisal University, Al Ahsa-31982, SAUDI ARABIA.
Email: graza@kfu.edu.sa

Received: 16-01-2025;
Revised: 04-03-2025;
Accepted: 28-05-2025.

INTRODUCTION

The human unicellular protozoan parasite *Plasmodium falciparum* (*P. falciparum*) is the noxious species of Plasmodium that causes malaria in humans.[1,2] A female Anopheles mosquito bite transmits the parasite that causes falciparum malaria, the most severe type of the illness. It is the cause of around half of all cases of malaria. *P. falciparum* is therefore believed to be the most lethal parasite that infects humans.[3] *P. falciparum* is the relevant agent of practically all malarial fatalities, with 95% of cases happening in Africa. *P. falciparum* was the cause of closely all cases in Sub-Saharan Africa; in contrast, other, less virulent species are more collective in most other malarial countries.[4] Since a single cell can alteration its DNA up to a million times a day, DNA lesions pose a continuous danger to the integrity of the genome.[5] Prokaryotic and eukaryotic organisms have progressed a stringent system of checks and balances using the DNA repair machinery in order to maintain this genomic integrity. Several proteins involved in DNA repair processes such as NER (Nucleotide Excision Repair) MMR, (Mismatch Repair) and BER (Base Excision Repair), have undergone significant evolutionary conservation in both prokaryotic and eukaryotic organisms.[6] While the basic concept remains the same, NER in eukaryotes is more complex than in prokaryotes. NER implicates the assembly of proteins that distinguish, cut, and extract the broken strand from the genomic DNA.

In accumulation to transcription, the multifunctional cellular Transcription Initiation Factor IIH (TFIIH) is concerned in NER. The Cdk-Activating Kinase Module (Cak), which is prepared up of the three subunits Cdk7, cyclin H, and MAT1, is related to the core of the mammalian TFIIH, which is made up of the seven subunits p52, XPB, p34, XPD, p62, p44, and p8/TTD-A.[7-9] Through its connotation with RNA polymerase II,

DOI: 10.5530/ijper.20251797

TFIIH shows a part in transcription. According to information, RNA polymerase II-mediated transcription and maybe NER are inhibited when the enzymatic activities of human XPB are reduced.[10] Numerous studies designate that transcriptional controls are significant for controlling gene expression during the life cycle of *P. falciparum*.[11] We hypothesize that disruption of the NER system in combination with other DNA repair processes may be the cause of *P. falciparum* drug resistance. Therefore, we decided to use bioinformatics-based methods to break down the *P. falciparum* NER route into its component pieces. As we know that due to continuous use of available drugs such as Chloroquine phosphate, Artemisinin-based combination therapies, Atovaquone-proguanil, Quinine sulfate and Primaquine phosphate, these drugs become resistance, therefore urgent need for the identification of novel drugs for the treatment of malaria. In the present *in silico* and *in vivo* study, the effect of various antitumor ligands (etoposide, novobiocin, netropsin, daunorubicin, and nogalamycine (Figure 1). Here, we explore the interactions between the target protein with the antitumor drugs Etoposide, Novobiocin, Netropsin, Nogalamycin and Daunorubicin. *In vivo* study was to analyze the activity of the compound's inhibition under SYBER Green dye fluorescence screening method to find out which antitumour drug is moreaffective on parasite growth.

MATERIALS AND METHODS

Docking and ADMET Analysis

The optimization of ligands 1-5 i.e., Etoposide (ligand 1), Novobiocin (ligand 2), Netropsin (ligand 3), Nogalamycin (ligand 4) and Daunorubicin (ligand 5) was conducted using the DFT/M06-2X/6-311G level of theory within the Gaussian16 software package.[12-15] The research of the interactions between the target protein {PF3D7_1441900 (transcription factor TFIIH complex subunit Tfb5, putative) *P. falciparum* (isolate 3D7)} and the ligands 1-5 were performed by using the AutoDock Vina program and AutoDock-Tools (ADT).[16] The prediction and modelling of protein was carried out by using the I-Tasser platform.[17] The water molecules were removed before performing the docking. When assigning both grid box sizes, (40 × 40 × 40 Å centered at X=62.833, Y=57.677, Z=60.815), the residues of each protein's active site were taken into account. The Biovia Discovery Studio Visualizer 2021 was used to visualize the ligand-protein interactions and docked poses.[18] Pharmacokinetic property of all the five ligands was also performed by using the ADMET 2.0 (https://admetmesh.scbdd.com).

Parasite Culture

The effects of the antitumor drugs were investigated using cultures containing 1% infected Red Blood Cells (RBCs) and 4% hematocrit. After centrifuging the parasite culture, drugs were applied. The parasite culture mixture was placed in 96-well plates and cultured for varying time periods at 37°C. The erythrocytic phases of the parasite development were used to prepare the smears at various time intervals. Slides were then fixed for 20 sec in methanol. After that, it was dyed for 30 min by dipping it in Sigma's diluted factor (1:20) Giemsa stain. A thorough microscopic examination of slides submerged in oil following cleaning and drying was conducted to analyze the cultures' morphology. After that, pictures were taken using a bright field microscope. Along with microscopic analysis, a SYBR green-based assay was carried out to look at the effect.[19]

Screening of antitumor drugs (Ligands 1-5) on parasite growth

This technique examined the connection between the fluorescence of the SYBER Green dye and the parasite. The standard procedure was used to remove *P. falciparum* from the parasite culture. Successively diluting the parasite concentration with water free of DNase was a series of dilutions. First, we used 40 µM of Etoposide, Novobiocin, Netropsin, Nogalamycin, and Daunorubicin to screen anticancer drugs (Ligands 1-5) on the *P. falciparum 3D7* cells. Additionally, we incubated the *P. falciparum* 3D7 cultures with SYBER Green dye after treating them with various concentrations (0.5 to 50 µM) of anticancer drugs (Etoposide and Novobiocin) and a control that included DNase-free water. Intensity was evaluated after incubating plates for an hour at Room Temperature (RT) in the dark. Plotting of fluorescence units versus parasite concentration was then done. An ELISA reader was used to take the SYBR green-based assay reading, and the parasite inhibition assay duplicates were conducted. Excel was used for plotting the graph. The effective growth inhibition of parasite cultures treated with novobiocin and etoposide is displayed in the bar graph.

RESULTS

Optimized structure of ligands 1-5

We have optimized all the five antitumor drugs Etoposide, Novobiocin, Netropsin, Nogalamycin and Daunorubicin to gain in-depth knowledge and understand their molecular properties for the expected requests. The optimized three-dimensional geometries of ligands 1-5 are shown in Figure 2.

Frontier Molecular Orbitals (HOMO-LUMO)

Figure 3 clearly shows the HOMO and LUMO of ligands 1-5 as well as the energy gap between their frontier orbitals. The EHOMO-LUMO gap of etoposide, novobiocin, netropsin, nogalamycin and daunorubicin is computed to be 5.31 eV, 4.66 eV, 5.10 eV, 3.48 eV and 3.58 eV and these results predict that the electron can transfer from HOMO to LUMO faster in case of Nogalamycin.

Molecular Electrostatic Potential (MEP) maps

Here, we have computed the MEPs of all the five ligands which are revealed in Figure 4. The computed possible value is found to be -7.159 x 10^{-2}, -8.734 x 10^{-2}, -6.465 x 10^{-2}, -8.259 x 10^{-2}, and -8.151 x 10^{-2} for the ligands 1-5, respectively. Computed values of the MEPs for five ligands reveal specific values, with ligand 2 exhibiting the most negative potential and ligand 3 displaying the least negative potential. Further analysis shows that the reddish hues predominantly surround oxygen atoms, indicating a likelihood of electrophilic attack, while yellowish shades cluster around nitrogen atoms, suggesting a predisposition for nucleophilic attack.

Molecular docking Analysis

The docked models were analyzed to determine the binding affinities and types of intermolecular bonding interactions between each ligand and the target proteins. By examining their preferred binding orientations, various ligand interactions with proteins were identified. Compounds that exhibited strong interactions with the target protein were considered successful in the docking process. Additionally, the impact of different docking postures and energies on the docking outcomes was observed and evaluated.

The different binding energy values gotten from the docking result of all the five ligands are shown in Table 1. Our study predicted that all the five ligands exhibit binding interactions with the target protein. The 3d and 2d structures showing ligands-protein interactions of ligands 1-5 are shown in Figures 4A-E, respectively. The binding affinity values of nine different binding modes of ligand with proteins obtained from the docking results are -6.4, -6.4, -5.9, -5.9, -5.9, -5.8, -5.7, -5.7, -5.7 kcal/mol, (see Figure 5A), correspondingly. The docking conformation with the lowest (most negative) binding energy value indicates the maximum binding affinity. The observed interactions of notable significance encompassed hydrogen bonding, π-π stacking, π-cation, π-sigma, π-sulphur and π-alkyl interactions. The H-bonding is present at a distance of range 2.10-2.60 Å. Two prominent interactions, namely π-sigma and π-cation are observed at a range of distances 4.20-4.55 Å and 4.50-4.80 Å, respectively. The docking results reveal that ligands 1-5 exhibit most negative binding energy values of -6.4, -6.5, -5.8, -6.0, and -6.2 kcal/mol, respectively, indicating their highest binding affinity in this mode. A comprehensive summary of the binding affinities values for ligands 1 to 5 is shown in Table 1. Important interactions that have been noted between amino acid residues and ligand 3 include H-bonding, π-alkyl, π-sigma, π-cation, and alkyl-alkyl interactions which appear at distances of 2.54 Å, 3.68 Å, 4.41 Å, 2.59 Å and 4.22 Å, respectively as shown in Figure 5B.

Likewise, the dominant interactions seen in the subsequent ligand. Ligands 1 and 2 exhibit equivalent minimal relative interaction energies within the given set. The interaction energy of ligand 3 is comparatively lower, therefore, showing a relatively lower affinity for binding to proteins. On the other hand, ligands 1 and 2 exhibit higher binding energies, which implies that they are more efficient at binding to proteins. Among all ligands, ligand 2 has the highest binding energy, indicating its highest efficiency to bind with proteins. It has been found that hydrogen bonding, π-cation, π-alkyl and π-sigma interaction have played a critical role in linking the ligands with protein.

ADME Analysis

Through this platform, we gain valuable insights into how the drug behaves in the body, aiding in informed decisions about its potential for advancement. Using this platform, we gain extensive insights into how the drug operates within the body, enabling well-informed decisions about its potential progression. The absorption aspect encompasses various parameters, including Caco-2 Permeability, MDCK Permeability, Pgp-inhibitor, Pgp-substrate, HIA, F20%, and F30%. Caco-2, a human colon adenocarcinoma cell line, is utilized to assess drug permeability.

Table 1: Binding affinity values of ligands (Antitumor Drugs) 1-5.

Mode	Etoposide (ligand 1) Affinity (kcal/mol)	Novobiocin (ligand 2) Affinity (kcal/mol)	Netropsin (ligand 3) Affinity (kcal/mol)	Nogalamycine (ligand 4) Affinity (kcal/mol)	Daunorubicin (ligand 5) Affinity (kcal/mol)
1	-6.4	-6.5	-5.8	-6.0	-6.2
2	-6.4	-6.3	-5.8	-5.9	-6.1
3	-5.9	-6.1	-5.6	-5.8	-6.0
4	-5.9	-5.8	-5.5	-5.8	-6.0
5	-5.9	-5.8	-5.2	-5.7	-6.0
6	-5.8	-5.8	-5.2	-5.6	-6.0
7	-5.7	-5.7	-5.2	-5.6	-6.0
8	-5.7	-5.7	-5.2	-5.4	-5.8
9	-5.7	-5.6	-5.0	-5.3	-5.8

The prediction of Caco-2 permeability is represented as the logarithm of centimeters per second (log cm/s). A value higher than -5.15 log cm/s indicates sufficient permeability. MDCK cells are employed to evaluate chemical absorption and predict its impact on the blood-brain barrier. The permeability coefficient (Papp) is measured in cm/s, where a value greater than 2 x 10^{-6} cm/s signifies outstanding permeability.

A Pgp-inhibitor is a compound that hinders the function of P-glycoprotein, known for its role in identifying various xenobiotics, many of which are substrates of CYP3A4. The Pgp-inhibitor probability score ranges from 0 to 1, where a score between 0 and 0.3 is considered excellent, 0.3 to 0.7 denotes medium, and 0.7 to 1.0(++) indicates poor inhibition. Altering P-glycoprotein transport significantly affects the pharmacokinetics of substances identified by Pgp, potentially leading to therapeutic effects or contraindications. The likelihood of being a Pgp substrate is indicated by output values between 0 and 1. Scores falling within 0 and 0.3 indicate excellent probability, while those between 0.3 and 0.7 suggest medium probability, and scores between 0.7 and 1.0 indicate poor probability. Human Intestinal Absorption (HIA) is pivotal in determining the effectiveness of orally administered medications.

Human intestinal absorption analysis

Studies indicate a strong correlation between oral bioavailability and intestinal absorption, making HIA a crucial indicator of bioavailability. A molecule with less than 30% absorption is typically classified as poorly absorbed. The output value indicates the likelihood of having Human Intestinal Absorption (HIA+),

Table 2: ADME analysis for ligands 1-5.

Properties	Etoposide (ligand 1)	Novobiocin (ligand 2)	Netropsin (ligand 3)	Nogalamycin (ligand 4)	Daunorubicin (ligand 5)
MW	588	612	466	665	527
H-bond acceptors	13	13	13	14	11
H-bond donors	3	6	10	8	6
Rotatable bond	5	10	11	3	4
TPSA	160	200	213	230	185
Log S	-3.6	-3.7	-2.5	-2.8	-4.1
Log P	1.4	3.7	-1.8	-0.7	2.4
Caco-2 Permeability	-5.5	-5.7	-5.7	-5.9	-6.0
MDCK Permeability	5.7e-05	8.2e-06	1e-05	0.00012	6.1e-06
Pgp-inhibitor	---	-	---	---	+++
Pgp-substrate	+++	+++	+++	+++	+++
HIA	---	--	---	++	++
F20%	---	---	+++	+++	++
F30%	---	+++	+++	+++	+++
PPB	91%	87%	47%	25%	94%
VD	0.4	0.6	1.6	0.3	1.0
BBB Penetration	---	---	++	--	---
Fu	7.0%	7.1%	7.1%	13.3%	3.9%
CYP1A2 inhibitor	---	---	---	---	---
CYP2C19 inhibitor	---	---	---	--	---
CYP2C9 inhibitor	--	-	-	---	--
CYP2D6 inhibitor	---	-	-	---	---
CYP3A4 inhibitor	++	--	--	--	-
CL	4.9	3.6	3.6	1.3	18.6
T1/2	0.19	0.24	0.24	0.77	0.02

[MW=Molecular Weight, TPSA= Topological polar surface area, Log S= logarithm of aqueous solubility value, Log P= logarithm of the n-octanol/water distribution coefficient, Caco-2= human colon adenocarcinoma cell lines, MDCK= Madin–Darby Canine Kidney cells, Pgp= P-glycoprotein, HIA= Human intestinal absorption, F20%= human oral bioavailability 20%, F30%= human oral bioavailability 30%, PPB= Plasma protein binding, VD=Volume Distribution, BBB= blood–brain barrier, Fu= fraction unbound, CL= clearance of a drug, $T_{1/2}$= half-life of a drug. For the classification endpoints, the prediction probability values are transformed into six symbols: 0-0.1(---), 0.1-0.3(--), 0.3-0.5(-), 0.5-0.7(+), 0.7-0.9(++), 0.9-1(+++)].

ranging from 0 to 1. An excellent score falls within 0 to 0.3, medium probability ranges from 0.3 to 0.7, and a poor score is between 0.7 and 1.0 (++). F20% is a vital parameter for orally administered drugs, reflecting oral bioavailability at 20% and assessing the efficacy of systemic drug delivery. The output value, ranging from 0 to 1, denotes the probability of having F20%+. An excellent probability score lies between 0 and 0.3, medium probability ranges from 0.3 to 0.7, and a poor score is between 0.7 and 1.0 (++). Similarly, F30% represents oral bioavailability at 30%, crucial for evaluating drug delivery efficacy into the systemic circulation. Expressed as a percentage, molecules with over 30% bioavailability are deemed effective (F30%-). The output value provides the probability of being F30%+, ranging from 0 to 1. An excellent probability score is between 0 and 0.3, medium falls between 0.3 and 0.7, and a poor score ranges from 0.7 to 1.0 (++).

PBB, VD, BBB, Fu and PPB analysis

Distribution involves various parameters, including Plasma Protein Binding (PPB), Volume of Distribution (VD), Blood-Brain Barrier (BBB) Penetration, and Fraction Unbound (Fu).

Plasma Protein Binding (PPB) significantly influences a drug's uptake and distribution in the body. The interaction between a drug and plasma proteins directly affects its pharmacodynamic behavior. PPB also affects oral bioavailability by reducing the concentration of free drug available for action. Ideally, a compound's predicted PPB value should be less than 90% to maintain a suitable therapeutic index. Volume of Distribution (VD) is a crucial parameter describing how drugs disperse throughout the body. Expressed in Litres per Kilogram (L/kg), VD aids in predicting a compound's distribution characteristics, offering insights into its tissue distribution and pharmacokinetic profile. An appropriate Volume of Distribution (VD) typically ranges from 0.04 to 20 L/kg. Blood-Brain Barrier (BBB) penetration is vital for drugs targeting the Central Nervous System (CNS) to reach their intended site of action effectively. This metric, measured in Centimeters per Second (cm/s), ranges from 0 to 1. A score between 0 and 0.3 indicates excellent penetration, 0.3 to 0.7 denotes medium penetration, and 0.7 to 1.0 (++) suggests poor penetration. Drugs in plasma can exist in two forms: bound to serum proteins or unbound. Binding to proteins may potentially impede a drug's efficacy.

The Fraction Unbound (Fu) value indicates the percentage of unbound drug in plasma. A Fu value exceeding 20% is considered high, while 5% to 20% is categorized as medium, and less than

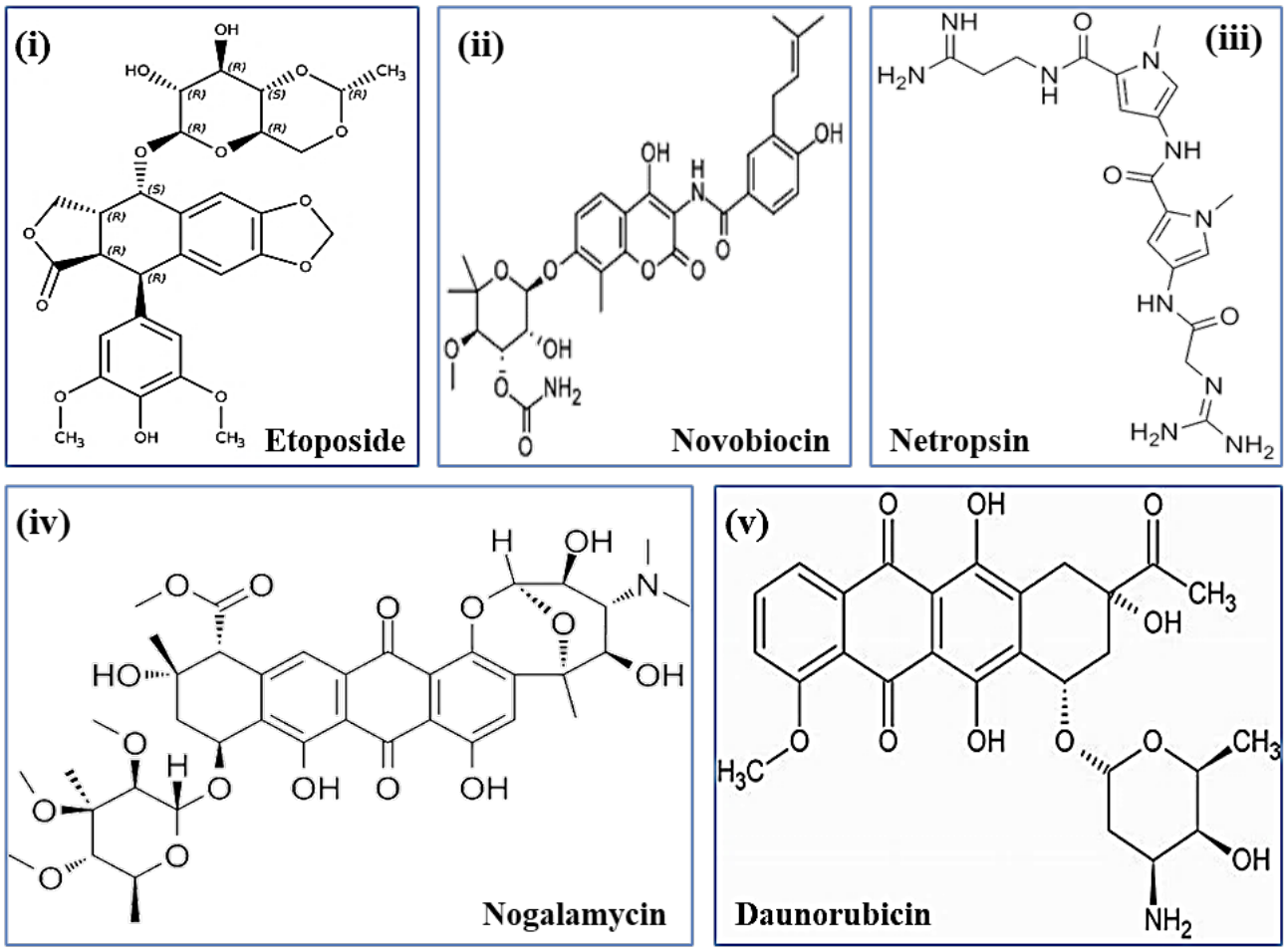

Figure 1: Chemical structures of antitumor drugs (i) Etoposide, (ii) Novobiocin, (iii) Netropsin, (iv) Nogalamycin and (v) Daunorubicin.

5% is deemed low. A Fu value of 5% or higher is regarded as outstanding, whereas less than 5% is considered poor. Metabolism involves assessing inhibition towards various cytochrome enzymes, including CYP 1A2, 2C19, 2C9, 2D6, and 3A4. Drug metabolism reactions are categorized into phase I (oxidative) and phase II (conjugative). The human cytochrome family, with 57 isozymes, plays a crucial role in metabolizing about two-thirds of known drugs in humans. Notably, five enzymes (1A2, 3A4, 2C9, 2C19, and 2D6) account for 80% of drug metabolism. Output values are represented as probabilities ranging from 0 to 1, indicating the likelihood of inhibition towards these key cytochrome enzymes.

Excretion involves two crucial parameters: drug Clearance (CL) and half-life (T1/2). Drug clearance is a significant determinant of a drug's effectiveness. Predicted clearance is measured in milliliters per minute per kilogram (mL/min/kg). Values above 15 indicate high clearance, while those ranging from 5 to 15 suggest moderate clearance, and values below 5 indicate low clearance. A clearance value of ≥ 5 is generally considered excellent, whereas a value below 5 is deemed poor. The half-life (T1/2) of a drug is influenced by its clearance and volume of distribution, representing the time needed for the drug concentration in the body to decrease by half. The obtained value ranges from 0 to 1, where 0 to 0.3 signifies excellent, 0.3 to 0.7 indicates medium, and 0.7 to 1.0 (++) suggests poor. The values from the ADME analysis are provided in Table 2.

The ADME analysis of ligand 1 reveals the following characteristics: it has thirteen hydrogen bond acceptors, three hydrogen bond donors, and five rotatable bonds. Adsorption analysis shows exceptional Caco-2 permeability (-5.5), strong P-glycoprotein (Pgp) inhibition (0-0.1), and low Pgp substrate potential (0.9-1). Human Intestinal Absorption (HIA), fraction absorbed at 20% (F20%), and fraction absorbed at 30% (F30%) are all within the excellent range (0-0.1).

Distribution analysis indicates a low Plasma Protein Binding (PPB) value of 91%, and it demonstrates excellent Volume of Distribution (VD) and Blood-Brain Barrier (BBB) penetration values (0-0.1). Additionally, its Fraction Unbound (Fu) is 7.0%. Metabolism analysis shows Ligand 1 as a good inhibitor of CYP1A2, CYP2C19, and CYP3A4, with values between 0 and

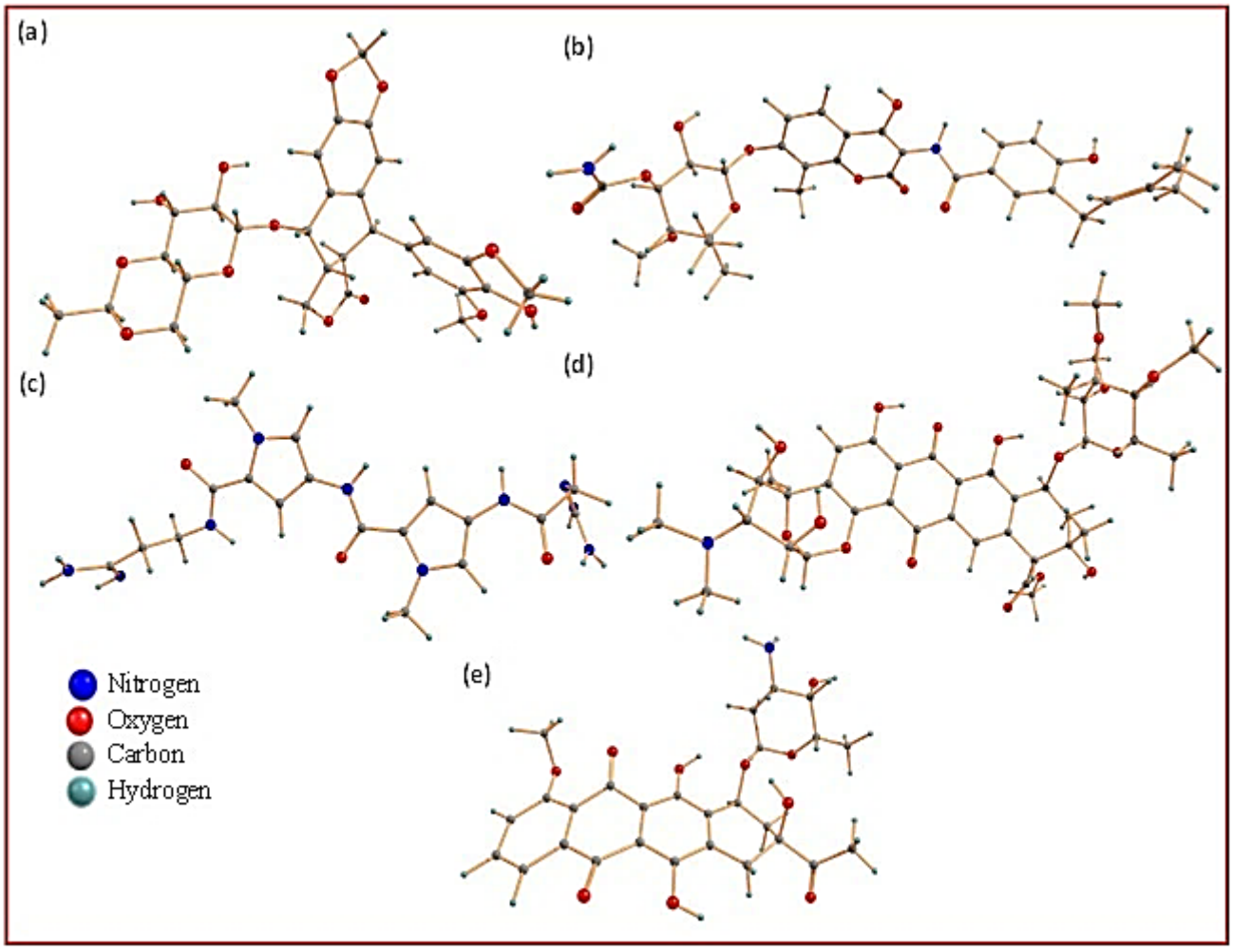

Figure 2: Optimized structures of (a) Etoposide (ligand 1), (b) Novobiocin (ligand 2), Netropsin (ligand 3), (d) Nogalamycin (ligand 4) and (e) Daunorubicin (ligand 5).

1, but it presents moderate inhibition for CYP2C9. Excretion analysis reveals a Low Clearance (CL) value of 4.955 and an excellent half-life (T1/2) value of 0.19.

Ligand 2 exhibits the following characteristics: it has thirteen hydrogen bond acceptors, six hydrogen bond donors, and ten rotatable bonds. Adsorption analysis shows excellent Caco-2 permeability (-5.7), no significant P-glycoprotein (Pgp) inhibition, and poor potential as a Pgp substrate (0.9-1). Human Intestinal Absorption (HIA), fraction absorbed at 20% (F20%), and fraction absorbed at 30% (F30%) are all within the excellent range (0-0.1). Distribution analysis indicates an excellent Plasma Protein Binding (PPB) value of 87%, and it demonstrates excellent Volume of Distribution (VD) and Blood-Brain Barrier (BBB) penetration values (0-0.1). Additionally, its Fraction Unbound (Fu) is excellent at 7.1%. Metabolism analysis shows ligand 2 as an excellent inhibitor of CYP1A2, CYP2C19, CYP2C9, CYP2D6, and CYP3A4, with values between 0 and 1. Excretion analysis reveals a Low Clearance (CL) value of 3.698 and an excellent half-life (T1/2) value of 0.24.

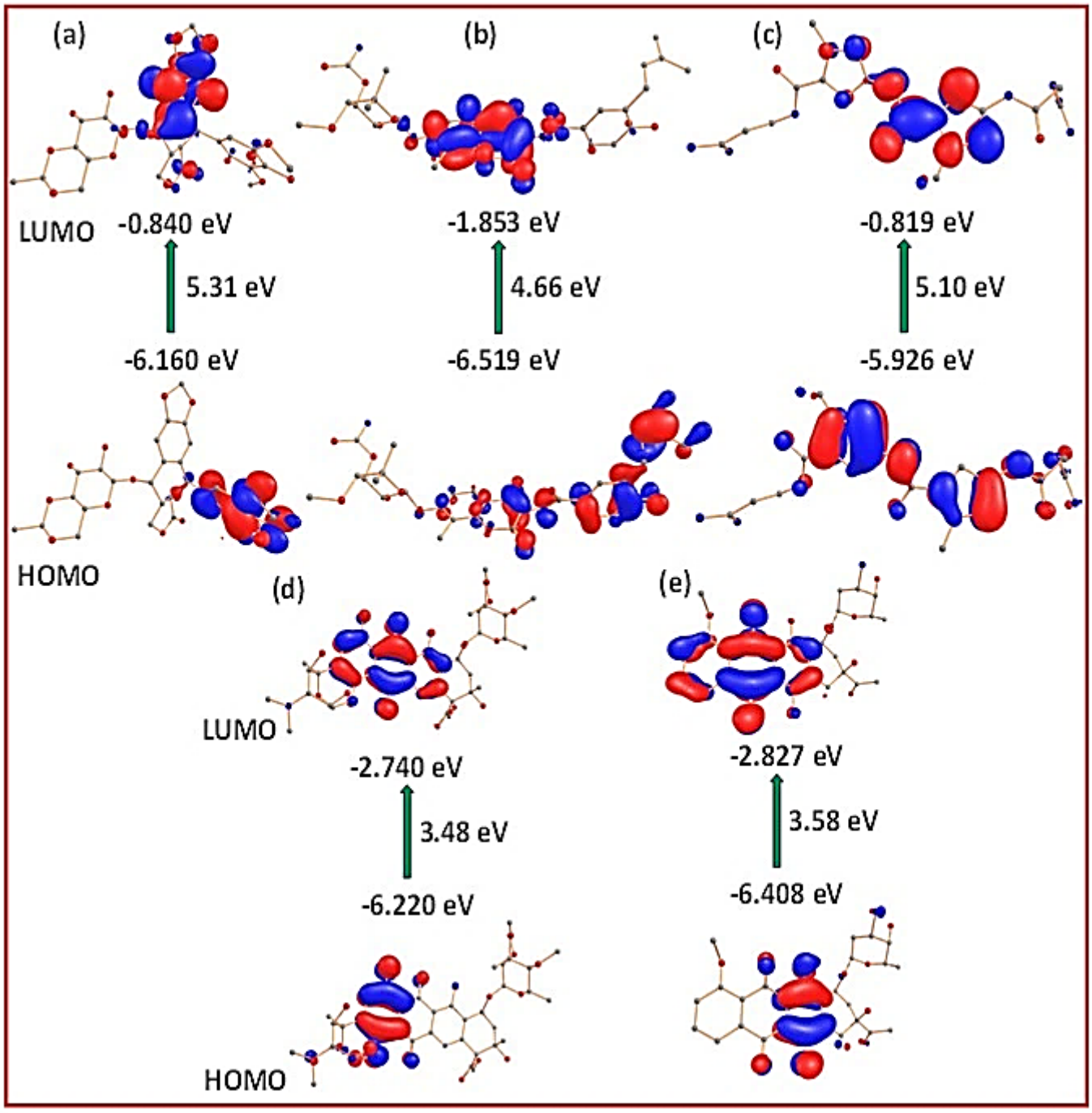

Figure 3: Figured HOMO-LUMO gap of (a) Etoposide (ligand 1), (b) Novobiocin (ligand 2), (c) Netropsin (ligand 3), (d) Nogalamycin (ligand 4) and (e) Daunorubicin (ligand 5).

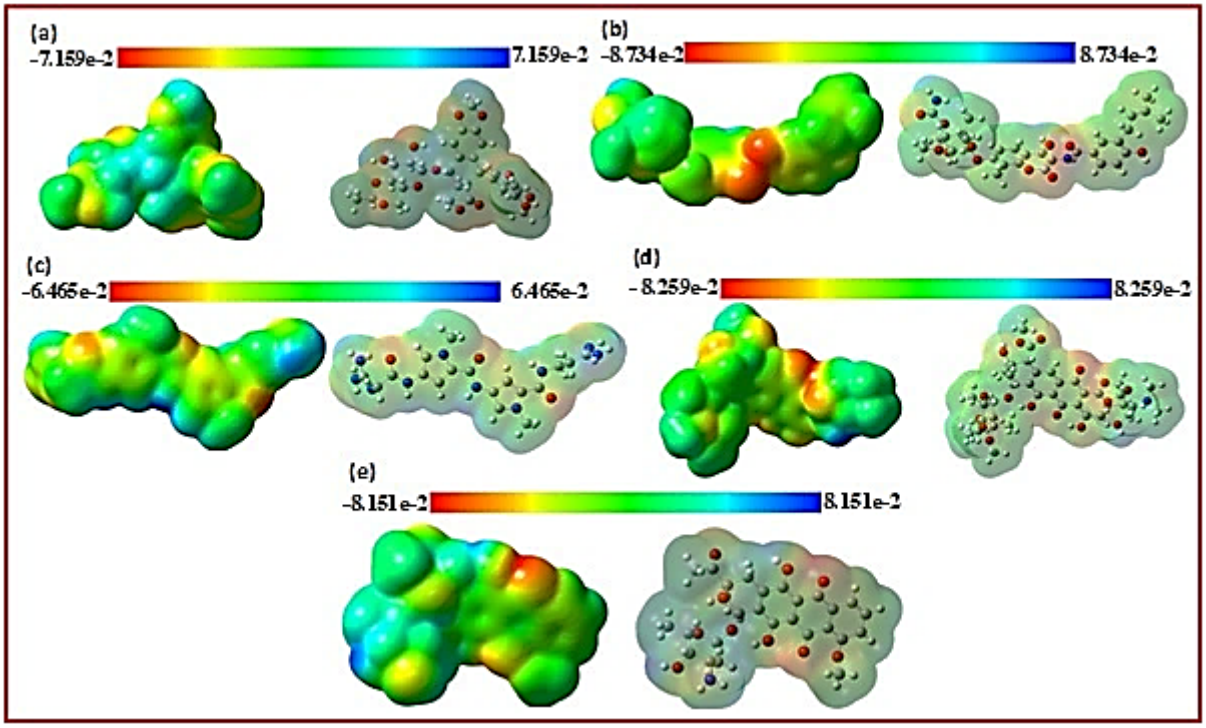

Figure 4: Computed MEPs of (a) Etoposide (ligand 1), (b) Novobiocin (ligand 2), (c) Netropsin (ligand 3), (d) Nogalamycin (ligand 4) and (e) Daunorubicin (ligand 5).

Ligand 3 possesses thirteen hydrogen bond acceptors, ten hydrogen bond donors, and eleven rotatable bonds. Adsorption analysis reveals excellent Caco-2 permeability (-5.7), excellent P-Glycoprotein (Pgp) inhibition, and poor potential as a Pgp substrate (0.9-1). Its Human Intestinal Absorption (HIA) value is excellent, while its fraction absorbed at 20% (F20%) and fraction absorbed at 30% (F30%) values are poor (0.9-1). Distribution analysis indicates excellent Plasma Protein Binding (PPB) at 47%, an excellent Volume of Distribution (VD) value of 1.608, poor Blood-Brain Barrier (BBB) penetration, and an excellent Fraction Unbound (Fu) value of 7.1%. Metabolism analysis shows ligand 3 as an excellent inhibitor of CYP1A2, CYP2C19, CYP2C9, CYP2D6, and CYP3A4, with all values between 0 and 1. Excretion analysis reveals a Low Clearance (CL) value of 3.6 and an excellent half-life (T1/2) value of 0.24.

Ligand 4 exhibits the following characteristics: it has fourteen hydrogen bond acceptors, eight hydrogen bond donors, and three rotatable bonds. Adsorption analysis shows outstanding Caco-2 permeability (-5.9), excellent P-glycoprotein (Pgp) inhibition, and poor potential as a Pgp substrate (0.9-1). However, its Human Intestinal Absorption (HIA), fraction absorbed at 20% (F20%), and fraction absorbed at 30% (F30%) values are all within the poor range (0.7-0.9 and 0.9-1, respectively). Distribution analysis indicates excellent Plasma Protein Binding (PPB) at 25%, along with excellent Volume of Distribution (VD) and Blood-Brain Barrier (BBB) penetration values (0.3 and 0.1-0.3, respectively). Additionally, its Fraction unbound (Fu) is excellent at 13.3%. Metabolism analysis shows ligand 4 as an excellent inhibitor of CYP1A2, CYP2C19, CYP2C9, CYP2D6, and CYP3A4, with values between 0 and 1. Excretion analysis reveals a Low Clearance (CL) value of 1.3 and an excellent half-life (T1/2) value of 0.77.

Ligand 5 exhibits specific molecular characteristics. It features six hydrogen bond acceptors, eleven hydrogen bond donors, and four rotatable bonds. In terms of its pharmacokinetic profile, its adsorption analysis indicates notable Caco-2 permeability (-6.017), limited inhibition of P-glycoprotein (Pgp), and low potential as a Pgp substrate (0.9-1). Its human intestinal absorption (HIA) is also suboptimal, along with poor values for fraction absorbed at 20% (F20%) and fraction absorbed at 30% (F30%). Regarding distribution, it demonstrates moderate Plasma Protein Binding (PPB) at 94.430%, an excellent Volume of Distribution (VD) of 1.011, and satisfactory penetration through the Blood-Brain Barrier (BBB). However, its Fraction unbound (Fu) value is high at 3.912%. Metabolically, ligand 5 proves to be a potent inhibitor of several cytochrome P450 enzymes, as well as CYP1A2, CYP2C19, CYP2C9, CYP2D6, and CYP3A4, with inhibition values ranging between 0 and 1. In terms of excretion, it exhibits a Low Clearance (CL) value of 18.697 and an impressive half-life (T1/2) value of 0.019, indicating prolonged presence in the body.

Screening of Antitumor Drugs

The effects of various compounds (40 µM) on parasite growth *in P. falciparum* were analyzed. In the presence of different drugs, the percentage of inhibition of the development of parasites was

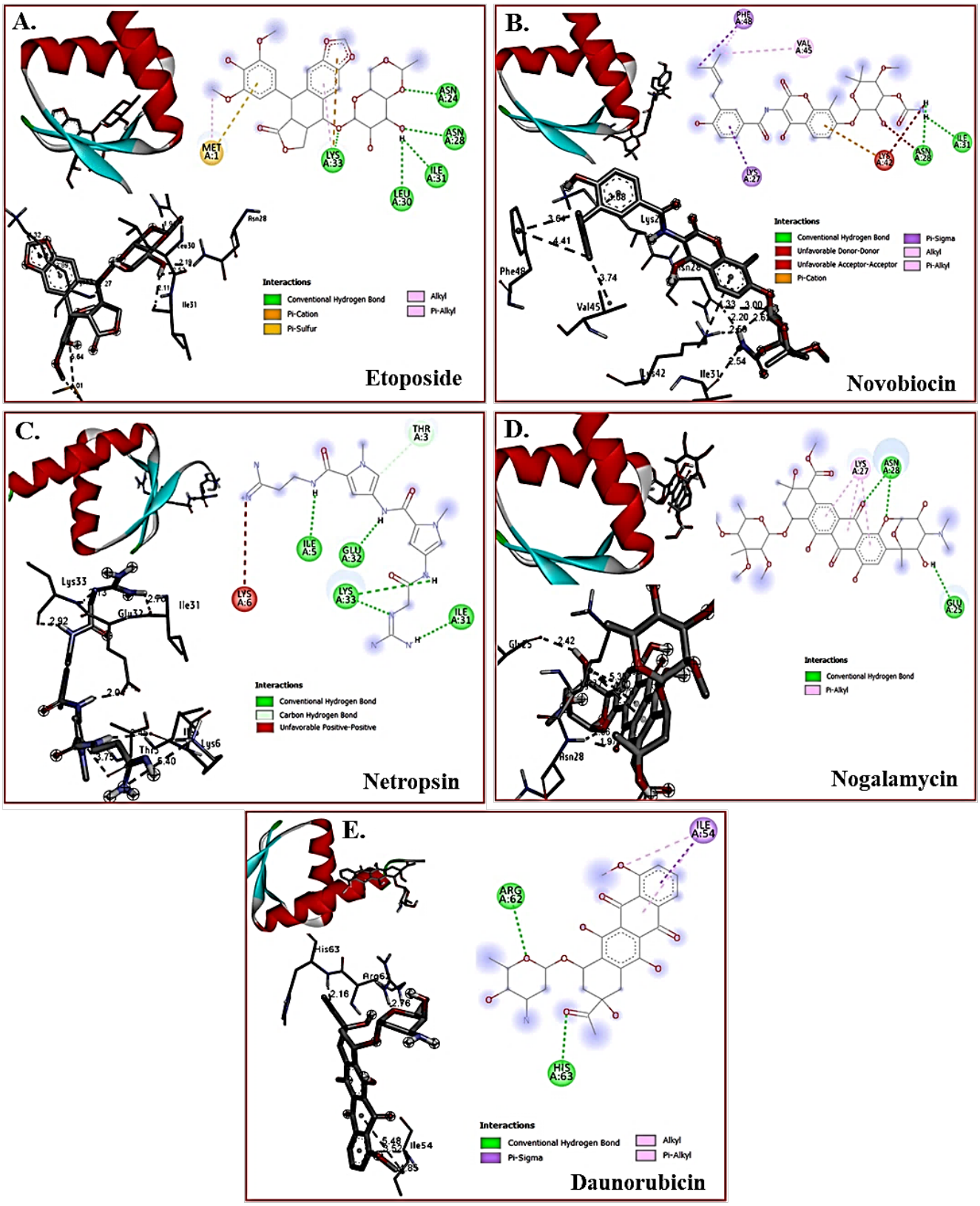

Figure 5: (A-E): 3D and 2D structures showing interactions between residues (amino acid) and species (1-5).

recorded. Parasitic growth is inhibited by 63% in etoposide, 71% and novobiocin, 45% in netropsin, 555 in nogalamycin, and 56% in daunorubicin. Results showed that novobiocin inhibits maximum amongst other drugs. At the same time, netropsin inhibits the lowest parasite growth (Figure 6A).

Effects of etoposide and novobiocin on parasite

In screening, we found that significant inhibition occurred in the presence of etoposide and novobiocin. We further performed the assay with increasing concentrations of etoposide and novobiocin with 0.5, 1.0, 2.5, 5.0, 10, 20, 30, 40, and 50 µM. We found that on 40 µM, the parasite inhibition will saturate (Figures 6B and C). The results show that the inhibition is high at 40 µM for etoposide and novobiocin. Among etoposide and novobiocin, novobiocin is significant drug in comparison to etoposide. The parasite inhibition observed in the presence of etoposide is 55% by using 50 µM, while novobiocin showed up to 69% by using 50 µ (Figures 6B and C). Thus, in the present study, we have identified that the ligand novobiocin showed maximum potential to inhibit *P. falciparum.*

DISCUSSION

A combined study involving Density Functional Theory (DFT) and molecular docking was performed to gain deeper insights into the reactivity, stability, and potential bioactivity of ligands**.** The molecular docking analysis revealed specific interactions between the investigated molecules and the amino acids within the target protein.[20-23]

Frontier molecular orbitals were studied, specifically the highest occupied and lowest unoccupied molecular orbitals, and the energy gap between them, which indicates ligands stability and reactivity.[24] A HOMO allows electrons to transfer to an

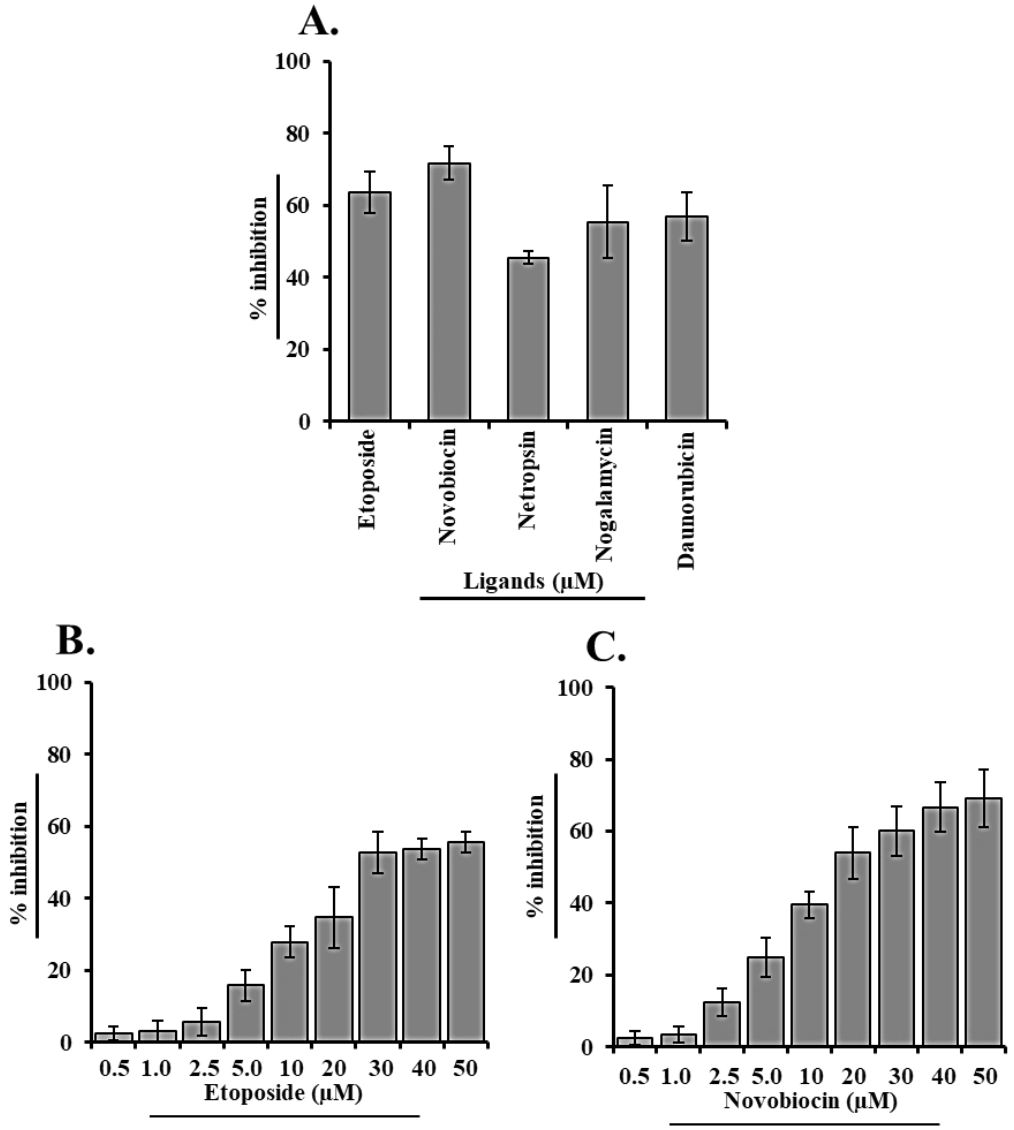

Figure 6: (A) Screening of Ligands 1-5 on parasite culture 3D7 strain. (B) Concentration dependents manner of Etoposide (C) Increasing concentration of Novobiocin. Graph was plotted by using excel.

unoccupied orbital, while a LUMO accepts them. It has been demonstrated that molecules with lower $E_{HOMO-LUMO}$ have greater bioactivity, and this can be used to explain the relative bioactivities of medicinal compounds.[25]

The molecular electrostatic potential highlights the positive and negative charges across the surface of molecules. It employs color coding to represent these charges: red signifies areas of high negative potential, blue indicates areas of high positive potential, and green and yellow represent the intermediary zones between these peaks. Through analysis, it's deduced that red regions denote negative potential, indicating a propensity for electrophilic attacks, while blue areas favor nucleophilic attacks. Intermediate shades denote areas where the potential is balanced between electrophilic and nucleophilic tendencies.

In silico ADME screening employs computational methods to predict the pharmacokinetic behavior of a prospective drug candidate. Pharmacokinetic attributes involve how the body interacts with a drug, including its absorption, distribution, metabolism, and excretion.[26-28]

The drug development process requires a deep understanding of how drugs interact with the human body. This involves predicting the drug's absorption rate into the bloodstream, its distribution throughout various tissues, its metabolic processes, and its eventual elimination. For this analysis, we utilize the ADMET 2.0 online servers accessible at (https://admetmesh.scbdd.com) which offer a comprehensive platform for assessing a drug candidate's pharmacokinetic properties.[29-32]

In experiments for *P. falciparum* growth suppression, the parasite is cultured in human erythrocytes and exposed to varying dosages of the potential anticancer drugs. Numerous techniques, such as flow cytometry, microscopy, and the Lactate Dehydrogenase (LDH) assay, can be used to quantify the inhibition of parasitemia. For instance, in *P. falciparum* cultures, doxorubicin, cisplatin, and etoposide have all demonstrated notable growth suppression, indicating their possible antimalarial action.[27]

Researchers frequently look into how effective anticancer medications affect particular biological pathways in the parasite, including as DNA replication, protein breakdown, and apoptosis, in order to ascertain its method of action. It has been demonstrated that proteasome inhibitors, such as bortezomib, specifically upset *P. falciparum* protein homeostasis, which results in parasite death.[28,29]

CONCLUSION

We have performed a theoretical study on five ligands such as Etoposide, Novobiocin, Netropsin, Nogalamycin and Daunorubicin to understand the behavior against the protein. We started the calculations with optimization of the ligands to get the stable geometry for further study. We have also studied the frontier molecular orbitals (HOMO-LUMO) and found that electron may transfer faster in ligand 4 followed by ligand 5, ligand 2, ligand 3 and ligand 1. We have also carried out a molecular docking study on etoposide, novobiocin, netropsin, nogalamycin and daunorubicin drugs with the target protein {PF3D7_1441900 *(*transcription factor TFIIH complex subunit Tfb5, putative*) P. falciparum* (isolate 3D7)}. Here we have studied nine different poses against the protein. The computed binding energy of etoposide, novobiocin, netropsin, nogalamycin and daunorubicin is found to be -6.4, -6.5, -5.8, -6.0, and -6.2 kcal/mol, respectively, indicates the ligand 2 has the highest binding energy which shows its highest efficiency to bind with proteins. Computed parameters of hydrogen bonding, π-cation, π-alkyl and π-sigma interactions during docking also played an important role in connection of etoposide, novobiocin, netropsin, nogalamycin and daunorubicin with the target protein. Further, the ADME analysis of ligands 1-5 provides valuable insights into their individual traits and potential applications. Ligand 1 stands out with exceptional permeability, distribution, and metabolism characteristics, making it a promising candidate for further investigation. Ligand 2 demonstrates strengths in absorption and metabolism, while ligand 4 exhibits potent inhibition of P-glycoprotein and metabolism-related properties. The analyses of ligands 3 and 5 emphasize their noteworthy distribution and metabolism features. Understanding these ADME profiles is crucial for evaluating the pharmacokinetic properties and possible uses of these compounds. Thus, in the present study, we have identified that the ligand novobiocin showed maximum potential to inhibit *P. falciparum*. Further exploration and research in this field could have significant implications for drug development and therapeutic approaches.

ACKNOWLEDGEMENT

All authors thank their institutes for the infrastructure support for this study.

CONFLICT OF INTEREST

The authors declare that there is no conflict of interest.

FUNDING

This work was supported by the Deanship of Scientific Research, Vice Presidency for Graduate Studies and Scientific Research, King Faisal University, Saudi Arabia [Grant No. KFU251850].

ABBREVIATIONS

RBCs: Red Blood Cells; **TFIIH:** Transcription Initiation Factor IIH; **RT:** Room Temperature, **ELISA:** Enzyme-Linked Immunosorbent Assay; **PPB:** Plasma Protein Binding; **VD:** Volume of Distribution; **BBB:** Blood-Brain Barrier; **Fu:** Fraction Unbound; **PPB:** Plasma Protein Binding; **CL:** Low Clearance; **DFT:** Density Functional Theory.

SUMMARY

A theoretical study on five ligands, including etoposide, novobiocin, netropsin, nogalamycin, and daunorubicin, was conducted to understand their behavior against the protein *P. falciparum*. The study found that ligand 4 had the fastest electron transfer, followed by ligand 5, ligand 2, ligand 3, and ligand 1. The molecular docking study revealed that ligand 2 had the highest binding energy, indicating its efficiency in binding with proteins. The ADME analysis of ligands 1-5 provided insights into their individual traits and potential applications. The study identified novobiocin as the most potent ligand to inhibit *P. falciparum*, with potential implications for drug development and therapeutic approaches.

REFERENCES

1. Rich SM, Leendertz FH, Xu G, Lebreton M, Djoko CF, Aminake MN, *et al.* The origin of malignant malaria. Proc Natl Acad Sci U S A. 2009; 106(35): 14902-7. doi: 10.1073/pnas.0907740106, PMID 19666593.
2. Perkins DJ, Were T, Davenport GC, Kempaiah P, Hittner JB, Ong'Echa JM. Severe malarial anemia: innate immunity and pathogenesis. Int J Biol Sci. 2011; 7(9): 1427-42. doi: 10.7150/ijbs.7.1427, PMID 22110393.
3. Perlmann P, Troye-Blomberg M. Malaria blood-stage infection and its control by the immune system. Folia Biol. 2000; 46(6): 210-8. PMID 11140853.
4. WHO. World malaria report 2021. Switzerland: World Health Organization. ISBN 978-92-4-004049-6; 2021.
5. Iben S, Tschochner H, Bier M, Hoogstraten D, Hozák P, Egly JM, *et al.* TFIIH plays an essential role in RNA polymerase I transcription. Cell. 2002; 109(3): 297-306. doi: 10.1016/s0092-8674(02)00729-8, PMID 12015980.
6. Coin F, Proietti De Santis LP, Nardo T, Zlobinskaya O, Stefanini M, Egly JM. p8/TTD-A as a repair-specific TFIIH subunit. Mol Cell. 2006; 21(2): 215-26. doi: 10.1016/j.molcel.2005.10.024, PMID 16427011.
7. Tajedin L, Anwar M, Gupta D, Tuteja R. Comparative insight into nucleotide excision repair components of Plasmodium falciparum. DNA Repair. 2015; 28: 60-72. doi: 10.1016/j.dnarep.2015.02.009, PMID 25757193.
8. Chigançaş V, Lima-Bessa KM, Stary A, Menck CF, Sarasin A. Defective transcription/repair factor IIH recruitment to specific UV lesions in trichothiodystrophy syndrome. Cancer Res. 2008; 68(15): 6074-83. doi: 10.1158/0008-5472.CAN-07-6695, PMID 18676829.
9. Nishiwaki T, Kobayashi N, Iwamoto T, Yamamoto A, Sugiura S, Liu YC, *et al.* Comparative study of nucleotide excision repair defects between XPD-mutated fibroblasts derived from trichothiodystrophy and xeroderma pigmentosum patients. DNA Repair. 2008; 7(12): 1990-8. doi: 10.1016/j.dnarep.2008.08.009, PMID 18817897.
10. Pascal JM, Tsodikov OV, Hura GL, Song W, Cotner EA, Classen S, *et al.* A flexible interface between DNA ligase and PCNA supports conformational switching and efficient ligation of DNA. Mol Cell. 2006; 24(2): 279-91. doi: 10.1016/j.molcel.2006.08.015, PMID 17052461.
11. van der Spek PJ, Smit EM, Beverloo HB, Sugasawa K, Masutani C, Hanaoka F, *et al.* Chromosomal localization of three repair genes: the xeroderma pigmentosum group C gene and two human homologs of yeast RAD23. Genomics. 1994; 23(3): 651-8. doi: 10.1006/geno.1994.1554, PMID 7851894.
12. Zhao Y, Truhlar DG. Density Functional for Spectroscopy: no long-range self-interaction error, good performance for Rydberg and charge-transfer states, and better performance on average than B3LYP for ground states. J Phys Chem A. 2006; 110(49): 13126-30. doi: 10.1021/jp066479k, PMID 17149824.
13. Ditchfield R, Hehre WJ, Pople JA. Self-consistent molecular-orbital methods. ix. An Extended Gaussian-Type Basis for Molecular-Orbital Studies of Organic Molecules. J Chem Phys. 1971; 54(2): 724-8. doi: 10.1063/1.1674902.
14. Becke AD. Density-functional thermochemistry. I. The effect of the exchange-only gradient correction. J Chem Phys. 1992; 96(3): 2155-60. doi: 10.1063/1.462066.
15. Frisch MJ, Trucks GW, Schlegel HB, Scuseria GE, Robb MA, Cheeseman JR, *et al.* 2016. Gaussian16, revision A.03. Gaussian, Inc., Wallingford CT.
16. Trott O, Olson AJ. AutoDock Vina: improving the speed and accuracy of docking with a new scoring function, efficient optimization, and multithreading. J Comp Chem. 2010; 31(2): 455-61. doi: 10.1002/jcc.21334, PMID 19499576.
17. Roy A, Kucukural A, Zhang Y. I-TASSER: a unified platform for automated protein structure and function prediction. Nat Protoc. 2010; 5(4): 725-38. doi: 10.1038/nprot.2010.5, PMID 20360767.
18. BIOVIASystemes, Dassault. San Diego: Dassault Systemes; 2021. [BIOVIA Discovery Studio].
19. Vydyam P, Chand M, Gihaz S, Renard I, Heffernan GD, Jacobus LR, et al. *In vitro* efficacy of next-generation dihydrotriazines and biguanides against babesiosis and malaria parasites. Antimicrob Agents Chemother. 2024; 68(9): e0042324. doi: 10.1128/aac.00423-24, PMID 39136469.
20. Azam M, Barik SR, Mohapatra PK, Kumar M, Ansari A, Mohapatra RK, *et al.* A bowl-shaped zinc-salen complex: structural analysis and molecular docking studies against omicron-s and delta-s variants. Russ J Inorg Chem. 2023; 68(8): 1005-12. doi: 10.1134/S0036023623600740.
21. Sahu R, Mohapatra RK, Al-Resayes SI, Das DK, Parhi PK, Rahman S, *et al.* An efficient synthesis towards the core of Crinipellin: TD-DFT and docking studies. J Saudi Chem Soc. 2021; 25(2). doi: 10.1016/j.jscs.2020.101193.
22. Sýs M, Kocábová J, Klikarová J, Novák M, Jirásko R, Obluková M, *et al.* Comparison of mononuclear and dinuclear copper (II). Dalton Trans. 2022; 51(36): 13703-15. doi: 10.1039/d2dt01610a, PMID 36001067.
23. Al-Shemary RK, Mohapatra RK, Kumar M, Sarangi AK, Azam M, Tuli HS, *et al.* Synthesis, structural investigations, XRD, DFT, anticancer and molecular docking study of a series of thiazole-based Schiff base metal complexes. J Mol Struct. 2023; 1275: 134676. doi: 10.1016/j.molstruc.2022.134676.
24. Ahamad MN, Shahid M, Ansari A, Kumar M, Khan IM, Ahmad M, *et al.* A combined experimental and theoretical approach to investigate the structure, magnetic properties and DNA binding affinity of a homodinuclear Cu(ii) complex. New J Chem. 2019; 43(19): 7511-9. doi: 10.1039/C9NJ00228F.
25. Varshney A, Mishra AP. Synthesis, spectral characterization, computational studies, antifungal, DNA interaction, antioxidant and fluorescence property of novel Schiff base ligand and its metal chelates. Spectrochim Acta A Mol Biomol Spectrosc. 2023; 297: 122765. doi: 10.1016/j.saa.2023.122765, PMID 37099994.
26. Mohapatra RK, Mahal A, Ansari A, Kumar M, Guru JP, Sarangi AK, *et al.* Comparison of the binding energies of approved mpox drugs and phytochemicals through molecular docking, molecular dynamics simulation, and ADMET studies: an *in silico* approach. J Biosaf Biosecur. 2023; 5(3): 118-32. doi: 10.1016/j.jobb.2023.09.001.
27. Ahmed M, Gupta MK, Ansari A. DFT and TDDFT exploration on the role of pyridyl ligands with copper toward bonding aspects and light harvesting. J Mol Model. 2023; 29(11): 358. doi: 10.1007/s00894-023-05765-4, PMID 37919553.
28. Da Silva MA, Veloso MP, de Souza Reis K, de Matos Passarini G, Dos Santos AP, do Nascimento Martinez L, et al. *In silico* evaluation and *in vitro* growth inhibition of Plasmodium falciparum by natural amides and synthetic analogs. Parasitol Res. 2020; 119(6): 1879-87. doi: 10.1007/s00436-020-06681-9, PMID 32382989.
29. Bieri C, Esmel A, Keita M, Owono LC, Dali B, Megnassan E, *et al.* Structure-based design and pharmacophore-based virtual screening of combinatorial library of triclosan analogues active against enoyl-acyl carrier protein reductase of *Plasmodium falciparum* with favourable ADME profiles. Int J Mol Sci. 2023; 24(8): 6916. doi: 10.3390/ijms24086916, PMID 37108083.
30. Muteeb G, Alsultan A, Farhan M, Aatif M. Risedronate and methotrexate are high-affinity inhibitors of New Delhi metallo-β-Lactamase-1 (NDM-1): A drug repurposing approach. Molecules. 2022; 27(4): 1283. doi: 10.3390/molecules27041283, PMID 35209073.
31. Muteeb G, Rehman MT, AlAjmi MF, Aatif M, Farhan M, Shafi S. Identification of a potential inhibitor (MCULE-8777613195-0-12) of New Delhi metallo-β-Lactamase-1 (NDM-1) using *in silico* and *in vitro* approaches. Molecules. 2022; 27(18): 5930. doi: 10.3390/molecules27185930, PMID 36144666.
32. AlAjmi MF, Rehman MT, Khan RA, Khan MA, Muteeb G, Khan MS, *et al.* Understanding the interaction between α-1-Acid Glycoprotein (AGP) and potential Cu/Zn metallo-drugs of benzimidazole derived organic motifs: A multi-spectroscopic and molecular docking study. Spectrochim Acta A Mol Biomol Spectrosc. 2020; 225: 117457. doi: 10.1016/j.saa.2019.117457, PMID 31450223.

Cite this article: Aatif M, Farhan M, Muteeb G. *In silico* and *in vivo* Evaluation of Antitumor Drugs against *P. falciparum* 3D7 Inhibit the Parasite Growth. Indian J of Pharmaceutical Education and Research. 2025;59(4):1522-33.